Published in final edited form as:
Nano Lett. 2010 January ; 10(1): 16–23. doi:10.1021/nl9023319.

Stabilization of Ion Concentration Polarization Using a Heterogeneous Nanoporous Junction

Pilnam Kim[1,†], **Sung Jae Kim**[2,†], **Jongyoon Han**[2,3,*], and **Kahp Y. Suh**[1,4,*]

[1]School of Mechanical and Aerospace Engineering, Seoul National University, Seoul, 151-742, Korea

[2]Department of Electrical Engineering and Computer Science, Massachusetts Institute of Technology, 77 Massachusetts Avenue, Cambridge, MA 02139, USA

[3]Department of Biological Engineering, Massachusetts Institute of Technology, 77 Massachusetts Avenue, Cambridge, MA 02139, USA

[4]World Class University Program on Multiscale Mechanical Design, Seoul National University, Seoul, 151-742, Korea

Abstract

We demonstrate a recycled ion – flux through heterogeneous nanoporous junctions, which induce stable ion concentration polarization (ICP) with an electric field. The nanoporous junctions are based on integration of ionic hydrogels whose surfaces are negatively- and positively- charged for cationic selectivity and anionic selectivity, respectively. It is shown that a 'heterojunction' structure with cationic selective hydrogels (CSH) and anionic selective hydrogels (ASH) can be matched up in a way to achieve continuous ion-flux operation for stable concentration gradient or ionic conductance. Furthermore, the combined junctions can be used to accumulate ions on a specific region of the device.

Ion transport through nano-scale geometries has been extensively studied due to its potential applications to biomolecule concentration[1-4] and separation[5, 6], fluid pumping [7] and switching[8], nanofluidic diode9, 10 and fuel cells11, [12]. In particular, ion concentration polarization (ICP) is important and useful in nanoscale ion transport, which can be generated by perm-selective transport through nanochannels or nanopores, because the Debye layer thickness (λ_D) is not negligible compared with the channel thickness in such small scale structures. As a consequence of overlapped electrical double layer (EDL) in nanochannels (typically < 50 nm), the ion perm-selective property creates an ion-flux imbalance between co- and counter-ions at the inlet and outlet of the nanoscale junction. One of the major challenges in homogeneous charged nanofluidic system is that the device must be operated under non-steady state conditions (with cation selective junction)[4, 13]. Under such systems, the ion depletion zone at the anodic side keeps ever-increasing, while the conductivity keeps decreasing until the depletion zone becomes unstable.14 Especially, the amplified electric field inside the depletion zone due to low electrical conductivity15 gave rise to an extremely fast vortical motion and this convective fluid motion mainly drives the instability.16, 17 In addition, ion enrichment at the cathodic side also leads to overall system instability in achieving efficient ICP18 [19]. In order to overcome many of these limitations, heterogeneous nanoporous junctions (with different polarity and different electroosmotic flow (EOF) direction) that are enable to

*Corresponding author: sky4u@snu.ac.kr: or jyhan@mit.edu.
†These authors equally contributed to this work.

match up the excess ions allows stable ionic currents to be maintained through the junction leading to stable operation. Despite its significant potential in various engineering applications, however, there are only a few examples of heterogeneously charged nanoporous junction that can exhibit ICP with either cation- or anion- perm-selectivity or both.

Hydrogels that are generated by polymeric cross-linking are attractive elements to nanoporous junction due to their response to specific stimuli, such as pH or temperature changes.[20-22] The properties of hydrogels are determined by various parameters including monomer composition, crosslinker density, and background ionic concentration.23 When the pore size of hydrogel matrix becomes comparable to the charge screening length (Debye length) and the gel exhibits many fixed charged groups, the hydrogel becomes a strong perm-selective material with preferential counter-ion conductances24. Compared with lithographically defined nanochannels[25, 26] and non-crosslinked polymer materials (such as Nafion®)27 these hydrogels can be structurally more robust, and cured into an arbitrary geometry and shape, thereby providing greater flexibility. Most importantly, the polarity of the materials and the surface charge density can be readily tuned, which is analogous to varying dopants (por n-types) and doping density in semiconductors.

Here, we investigated the effect of heterogeneously combined nanoporous junctions on the stability of ICP. It is shown that positively and negatively charged nanoporous junctions, under an applied electric field, are inducing ICP in the adjacent microchannel regions, with opposite polarity. More specifically, positively charged junctions induce ion depletion (enrichment) in the cathodic (anodic) side, as opposed to commonly used cation-selective nanoporous junctions. An application of both junctions in a microfluidic system allows one to demonstrate the effects of heterogeneous junction system on the stabilization of ICP, thereby introduceing a new concept for ‘ion collector system’.

To develop the ‘ion perm-selectivity’ attribute of the nanoporous junctions, we used positive and/or negative charged hydrogels, HEMA-AA for cation selective hydrogel (CSH), and DMAEMA for anion selective hydrogel (ASH) (see Methods and materials section). The ionic hydrogels were embedded inside the PDMS substrate, followed by irreversible sealing with the microchannel-patterned PDMS channel by plasma treatment, as shown in Figure 1a. These ionic hydrogels have been shown to present a fixed charge inside matrix at optimal pH conditions, owing to the deprotonation / protonation of acidic- / amine- groups[28]. The charge state of the chemical groups determines cationic or anionic perm-selectivity of the nanopores. The volume or nanopores size changes in this system, which is generated from swelling, would not be a significant factor, because the hydrogel is tightly confined within the micropatterned PDMS and strongly attached by oxygen plasma as shown in Figure 1b and 1c. Therefore, the swelling should be minimized compared to the volume change in an open-environment system[29], and the fluid flows through microchannels without physical interruption (from the swollen gel) as compared to previous approaches[30, 31]

In order to demonstrate a polarity of cationic selective hydrogel (CSH) junctions, we conducted measurements of ionic current density through the hydrogel nanoporous junction (width: 50 μm, depth: 10 μm) which connected two microchannels with three different ionic strengths; 1 mM, 10 mM and 100 mM KCl solutions as shown in Figure 2a. The microchannels used in CSH junction device had the dimension of 20μm height, 50μm width,, and 150μm spacing between each microchannel. A decrease in the ion currents as a function of time through nanoporous junctions under a dc bias is evidence of the formation of an ion depletion zone or the initiation of concentration polarization[14]. At low buffer concentration (for 1 mM and 10 mM), the current quickly dropped to its steady value, whereas it slowly decreased in the case of 100 mM because it takes longer to reach the proper thickness of EDL.

One of the important characteristic properties of ionic flow through nanoscale junction (or nanochannel) is that the ionic current versus applied voltage through the membrane has three distinguishable regions called Ohmic / limiting / over-limiting current regions.[32] At low voltages, the IV relation typical follows Ohm's law (Ohmic current region). At moderate voltages, the current can not increase linearly with the voltage due to an ion depletion zone at anodic side (limiting current region). In the over-limiting current region, the ionic current through perm-selective membrane significantly increases because of convective mixing inside ion depletion zone[14, 32]. We conducted another current measurement experiment for investigating the current behavior at three different ionic strength, 1 mM, 10 mM and 100 mM as shown in Figure 2b. Voltage, V, was swept from 0 V to 20 V at the rate of 0.1 V/30 sec across the junction. Since the hydrogel structure has highly negative charges by acrylic acid and the aforementioned effects, we can achieve three distinguishable regions even with 100 mM solution. Current studies have suggested that the model of the perm-selectivity of nano-scale structure originating from EDL overlap is not necessary the complete picture[14,33, 34] Rather, highly charged surface of nano structure can sustain (non-electroneutral) surface ion current, which can exist even when the equilibrium EDL is not 'overlapping' *per se*. This can be proven by the observation that depletion / enrichment can be generated even at high ionic strength (such as 100mM and even 1M), depending on the surface charge density of the nanojunction. Compared to silicon or glass device, the hydrogel can inherently have highly charged surface by adjusting the composition of charged additives. Thus, ICP can be initiated even with 100 mM solution in this hydrogel network device.

As a result, both the ion concentration and conductivity within the CSH decrease further, leading to higher perm-selectivity junction. In such cases, the overall ion current could drop to almost zero as shown in Figure 2a (their values were still non-zero because the applying voltage of 50 V can initiate "over-limiting current behavior" which imposes much higher current value than limiting current value), which can be viewed as analogous to a 'reverse bias' situation. In order to confirm the existence of both ion depletion/enrichment zones, ionic currents through either anodic- or cathodic- side microchannel were measured after applying an electric field through the nanoporous junction for a certain period of time (4 minutes for Figure 2c and 8 minutes for Figure 2d). Here, 1 mM KCl buffer solution was used for the measurement. This can be done by changing the voltage configuration from stage 1 (The voltage is applied through junctions) to stage 2 (The voltage is applied between the microchannel) (see the supplemental figure 2). As shown in Figure 2(a), the current reached its steady value within 20 sec, and thus 4 and 8 minutes were enough for obtaining steady current values. Moreover, this steady value largely depends on the (relatively high) resistance of depletion zone, not the (relatively low) resistance of enrichment zone. Thus, the constant current value before $t = 0$ (current value at the end of stage 1) can be confirmed by the initial current value of anodic side (depletion side), 3.66 nA for 4 min, and 3.16 nA for 8 min, (which are roughly the same) respectively. In the depletion zone, the initial low current increased up to the reference value which was measured through a microchannel having uniform electrolyte concentration. This is because the high resistance of depletion zone was getting lower as they flew and removed toward the reservoir. In this sense, the depletion (enrichment) zone was formed at the anodic (cathodic) side as shown in Figure 2c (Figure 2d) in the case of CSH junction. Also, the maintaining stage 1 longer can give higher enrichment factors as shown in Figure 2d as judged by higher initial current value at the cathodic side.

In the experiment, the cationic selective nanoporous junction (CSH, cationic selective hydrogel) and anionic selective nanoporous junction (ASH, anionic selective hydrogel) show opposite characteristics in the generation of ICP. Typically, surfaces charge distribution is one of critical factors in EOF [36]. In the case of CSH, the surface charge at CSH is negative, which induces the ion depletion zone formed at the anodic side, similar to lithographically defined nanochannel or Nafion nanojunction. The PDMS channel is also weakly negatively charged,

which leads to an overall electroosmotic flow toward the cathode, pumping the desalted (depleted) portion of fluid into the CSH junction. However, the situation with ASH junction is more complex due to the different surface charge of ASH and PDMS itself. Namely, EOF inside the ASH junction ($u_n^{EOF}=\mu_n\mathbf{E}$) points toward the anodic side, while EOF inside microchannel ($u_m^{EOF}=\mu_m\mathbf{E}$) points toward the cathodic side. The EOF magnitudes are mainly determined by spatial and temporal distribution of the surrounding electrolyte concentrations as shown in Figure 3a. Here, the electroosmotic mobilities (μ_n and μ_m) are functions of the zeta potential as well as **E**, i.e., the EOF velocity does not follow the Smoluchowski relation inside the depletion zone and nanoscale junctions.[15, 37] As shown in the inset of Figure 3b, the three different current regions (Ohmic, limiting, and overlimiting) are also observed in the case of ASH junction, and the ionic current through ASH junction initially dropped due to the formation of a depletion zone in the cathodic side. Here, the electrolyte concentration of 1 mM KCl solution was used. The reverse polarity of the ASH junction (depletion at cathodic side and enrichment at anodic side) can also be confirmed by fluorescent image tracking as shown in Figure 3c (at *t*=10sec). Ion enrichment at the anodic side decreases the electric field as well as the zeta potential in the microchannel (anodic side), therefore reducing u_m^{EOF}(EOF inside the microchannel). In addition, due to ion depletion in the cathodic side, both the zeta potential and the electric field increase, which increase u_n^{EOF} (EOF inside the nanoporous juncrions) The EOF generated within the ASH junction then becomes dominant ($u_m^{EOF} << u_n^{EOF}$), which makes the overall EOF to point toward the anode. From this moment, the depletion zone at the cathodic side is limited to a certain distance. As shown in the figure 3c at *t*=60 sec, the shape of depletion boundary is a convex lens rather than parabolic usually observed in a CSH device. This is because the overall flow field is subject to the competition between u_m^{EOF} (pushing toward cathodic reservoir) and u_n^{EOF} (pulling toward nanoporous junction). The overall current was measured increasing after 250 seconds as shown in Figure 3b. The ion-flux through each cathodic- and anodic- microchannel was also monitored by ion current. In this sense, enrichment behavior was observed at the anodic side and a depletion zone was created at the cathodic side. After maintaining stage 1 for 4 minutes, the current through cathodic/anodic microchannel followed typical depletion / enrichment situation, although with reversed polarity (cathodic depletion and anodic enrichment) as shown in Figure 3d. However, the same measurements at 8 minutes show much more complicated picture. The cathodic side microchannel current was measured to go above the reference current value as shown in Figure 3e, suggesting a substantial enrichment of ions on the cathodic channel (outside the observed depletion zone). Each reservoir at the end of anodic side can hold approximately 100 μL of buffer solution, and the portion of the fluid volume, which can possibly flow at least 30 minutes, was entirely enriched during the first 8 minutes of maintaining stage 1. Thus the current went up to the reference value (Figure 3e), while the current level with 4 minutes of stage 1 (Figure 3d) would not go above the reference value. Overall, the ion currents across the system were maintained near or above the steady state level, which is characteristically different from the CSH junction results. The opposite polarity of two different nanoporous junctions can lead to EOF with different direction in the device, which introduce a stable ion – flux within the device.

In order to test the opposite polarity of two difference nanojunction, we designed two different types of nanojunction devices: one is with junctions of the same charge (CSH-CSH junction) and the other with the oppositely charged junctions (CSH-ASH junction). The geometrical configuration of each device was identical (100 μm distance between each junction). Figure 4a shows the ionic current through the CSH-ASH hybrid junctions system with 1 mM KCl buffer solution. Initially, both the CSH and the ASH junctions operated and created ion ICP zones according to their own polarity, resulting in anodic depletion and cathodic enrichment as shown Figure 4b. However, as shown in Figure 4a, the overall ion current quickly returns to a steady state value that is only slightly lower than the ion current of uniform concentration. Therefore, the usual precipitous conductance drop, which is typically observed in devices using a single perm-selective nanochannels and nanopores, is not observed and a high level of

conductance is maintained. To investigate further details of ionic distribution both on the anodic and cathodic side, the currents through each side at (i) (4 minutes) and (ii) (18 minutes) were measured, as shown in Supplemental Figure 3a and 3b, respectively. The overall concentration profile in the cathodic (enrichment) and the anodic (depletion) side of the nanoporous junction is maintained. This is because ion enrichment (from the CSH junction) is mitigated by the action of the opposite ASH junction, which pumps extra anions to the opposite side. In order to verify the stabilization of ICP in the CSH-ASH hybrid nanoporous junction, green fluorescence protein (GFP) was introduced at both anodic and cathodic side. Oppositely charged ion tunnels can hinder or eliminate individual ionic transportation as shown in Figure 4c. Overall, the CSH junction is more conductive than the ASH junction, leading to cathodic enrichment and anodic depletion. This is because CSH junction (pKa=4.3 @ 25 °C) is more conductive than ASH junction (pKa=8.4) at this pH=7.4 condition. The CSH was approximately 2 times more conductive than ASH, as shown in the I-V slopes in the Ohmic regime of each nanoporous – junctions (Figure 2b for CSH and inset of Figure 3b for ASH). However, continuous concentration polarization is prevented by the current through ASH junction, mitigating any further ion concentration changes and maintains the size of the depletion / enrichment zones. As a result, ion current in this system reaches a steady state, which can be represented by the steady accumulation of molecules as a function of time. Such a condition was not obtained when two identical CSH junctions were used as shown in Figure 4d. This result clearly demonstrates that the advanced control of ion – flux can be obtained by integrating the opposite ion transport properties of CSH and ASH junctions. Also we performed experiments with various distances (50 μm, 100 μm, 500 μm, and 1 mm) between ASH and CSH. The results demonstrated that there was no interaction for a larger distance than 100 μm. It appeared that each junction acted independently and did not interact with each other based on the observation of the florescent images (See Supplemental Movie 3 where the gap between ASH and CSH is 1mm).

Some comments follow with regard to the advantageous aspect of hydrogels as an alternative to nanoporous junction device. It is worthwhile noting that the relative strength of the two opposite junctions can be tuned as needed, by changing the monomer composition of the hydrogel, or by increasing/decreasing the number of junctions. Such a manipulation would provide a new mode of ion – flux control, potentially leading to new device concepts. For example, one could build an ASH-CSH-ASH hybrid junction system, as shown in Figure 5. This system is ‘designed’ to have the dominant ion transport properties of ASH junctions, but with a CSH junction mitigating and maintaining the stability of the system (Figure 5a). Characterization of ion concentration distributions and overall ion transport behaviors are shown in Figure 5b~e. Here, the electrolyte concentration of 1 mM KCl solution was used. The unique feature of this system, as seen in Figure 5b, is that overall ion current through this system actually *increases* as a function of time, above the level predicted by uniform distribution of ions across the entire system. Also the weak ion depletion zone was initially formed at the cathodic side, while the strong enrichment zone was initially formed at the anodic side. This is similar behavior to the single ASH type junction because most of current pass through the shortest path, (along the left edge of the ASH hydrogel, which would form a least-resistance path between the left anodic reservoir and the left cathodic reservoir involved and vice versa) i.e. no current flow through center CSH. However, the weak depletion zone on the cathodic side (which was probably the limiting factor for the case of ASH-only junctions-Figure 3) was gradually eliminated and turned into an almost- uniform enrichment zone. The current through CSH junction in the middle may work to limit the extent of cathodic depletion zone. The overall conductance of the system continuously increased (i.e., working as an ‘ion collector’), since both side of the junction work as enrichment zones. This can be confirmed by current measurements in the microchannel, as shown in Figure 5c~5e. During the first 8~10 minutes, one can see that the initial polarization (both cathodic depletion and anodic enrichment) is slowly decreasing, while the concentration polarization is still local (shown by

the same steady state current of 30nA). However, by 18 minutes, it was shown that the weak depletion zone at the cathodic side (Figure 5c) was changed into the enrichment zone (Figure 5e). These effects gave rise to a higher ionic current through the nanoporous junctions without instability of ICP.

In summary, we have presented negative- and/or positive- charged nanoporous junctions inside microfluidics channel network by simple soft-lithographic integration and characterized the ICP phenomena in these complex systems. Utilizing this nanoporous junction system, we first demonstrated the reversed polarity of ICP in an anionic selective junction. This reversed polarity played a role in stabilizing the ICP by pumping anions to the opposite side, thus allowing for the generation of a controlled ion-pathway in an electrofluidic system. Such characterizations of hybrid nanoporous junction system (i.e., CSH-ASH and ASH-CSH-ASH) promise a great potential for manipulation of ions and biomolecules in various membrane applications, such in battery and desalination membranes.

Methods and materials section

Materials

Polydimethyl siloxane (PDMS) prepolymer and curing agent were purchased from Dow Corning (Sylgard 184). GFP for fluorescent tracking was purchased from CloneTech. For cationic selective hydrogels, a precursor mixture was used, consisting of 2-hydroxyethyl methacrylate (HEMA) and acrylic acid (AA) in the weight ratio of 5:1. The materials were purchased from Sigma-Aldrich Co. and vacuum-distilled prior to use. In the solution, a crosslinker (1 wt% ethylene glycol dimethacrylate (EGDMA)) and a photoinitiator (3 wt% 2,2-dimethoxy-2-phenyl-acetophenone(DMPA)) were used as the materials for photo-polymerizing (Signal-Aldrich Co.). The anionic selective hydrogel pre-polymer mixture consists of HEMA, 2-(dimethylamino)ethyl methacrylate (DMAEMA), EGDMA and DMPA in the weight ratios of 30.2:6.16:0.5:1.0, respectively.

Device Fabrication

To cure the PDMS prepolymer, a mixture of 10:1 silicone elastomer and curing agent was poured on various silicon masters prepared by photolithography and dry etching and placed at 60°C for 2 hr. The masters used for microfluidic channel had two branch channels with the dimension of 50 ~ 100 μm in width and 20 μm in height. The two channels were 100 μm apart. The maters used for hydrogel junctions had 50 μm in width, 10 μm in depth, and 100 μm in spacing between the adjacent junctions. Single or multiple channels were used depending on the construction geometry of the junction device. After curing, PDMS molds were cleanly detached from the masters. Glass slides were prepared by washing in distilled water and cleaned by plasma for 1 min. Initially, the acid and base monomers containing photo-curable hydrogels were pre-patterned on PDMS substrate, using the method called “micromolding in capillaries (MIMIC)”[38] The defined structure of hydrogel on PDMS surface was formed by rapid polymerization under ultraviolet (UV) light. Prior to introducing the hydrogel mixture, the pre-patterned PDMS channel was treated by controlled oxygen plasma, which allowed for strong adhesion between the pre-patterned PDMS surface and the cured hydrogel structure after polymerization. The conditions used were $t_{uv,\ HEMA\text{-}DMAEMA}$ = 60 s, and $t_{uv,\ HEMA\text{-}AA}$ = 40 s at a constant UV intensity of 10 mW/cm^2. The microfluidic PDMS channel and the bottom ionic-hydrogel embedded PDMS substrate were irreversibly bonded with O_2 plasma treatment for 60 s (PDC-32G, Harrick Scientific, Ossining, NY).

Electrokinetic Process

The ion depletion/enrichment zones were visualized by tracking fluorescence dye molecules and proteins that were added in the main 1 mM KCl solution at pH = 7.5. All the flow motions

and ion transport were imaged with an inverted fluorescence microscope (Olympus, IX-51) with CCD camera (SensiCam, Cooke corp.). Sequences of images were analyzed by Image Pro Plus 5.0 (Media Cybernetics inc.). A dc power supplier (Stanford Research System, Inc.) was used to apply an electrical potential to each reservoir through a homemade voltage divider. Keithley 236 Current/Voltage Source-Measure Unit (Keithley Instruments, Inc.) was used to measure the ionic current either through the hydrogel or microchannels

Supplementary Material

Refer to Web version on PubMed Central for supplementary material.

Acknowledgments

This work was supported by the Korea Science and Engineering Foundation (KOSEF) grant funded by the Korea government (MOST) (R01-2007-000-20675-0) and the Korean Research Foundation Grants funded by the Korean Government (MOEHRD) (KRF-2007-331-D00040 and KRF-J03000). This work was also partially supported by NIH (EB005743) and NSF (CBET-0347348).

References

1. Jung B, Bharadwaj R, Santiago JG. Analytical Chemistry 2006;78(7):2319–2327. [PubMed: 16579615]
2. Hlushkou D, Dhopeshwarkar R, Crooks RM, Tallarek U. Lab on a Chip 2008;8(7):1153–1162. [PubMed: 18584092]
3. Schoch RB, Han JY, Renaud P. Rev. Mod. Phys 2008;80(3):839–883.
4. Wang YC, Han JY. Lab on a Chip 2008;8(3):392–394. [PubMed: 18305855]
5. Schmidt-Rohr K, Chen Q. Nat. Mater 2008;7(1):75–83. [PubMed: 18066069]
6. Liu SR, Pu QS, Gao L, Korzeniewski C, Matzke C. Nano Letters 2005;5(7):1389–1393. [PubMed: 16178244]
7. Stone HA, Stroock AD, Ajdari A. Annual Review of Fluid Mechanics 2004;36:381–411.
8. Karnik R, Fan R, Yue M, Li DY, Yang PD, Majumdar A. Nano Lett 2005;5(5):943–948. [PubMed: 15884899]
9. Vlassiouk I, Siwy ZS. Nano Letters 2007;7(3):552–556. [PubMed: 17311462]
10. Daiguji H, Oka Y, Shirono K. Nano Letters 2005;5(11):2274–2280. [PubMed: 16277467]
11. Striemer CC, Gaborski TR, McGrath JL, Fauchet PM. Nature 2007;445(7129):749–753. [PubMed: 17301789]
12. Strickland DG, Litster S, Santiago JG. Journal of Power Sources 2007;174(1):272–281.
13. Lee JH, Song YA, Tannenbaum SR, Han J. Analytical Chemistry 2008;80(9):3198–3204. [PubMed: 18358012]
14. Kim SJ, Wang Y-C, Lee JH, Jang H, Han J. Phys. Rev. Lett 2007;99:044501. [PubMed: 17678369]
15. Kim SJ, Li L, Han J. Langmuir 2009;25(13):7759–7765. [PubMed: 19358584]
16. Zaltzman B, Rubinstein I. J. Fluid Mech 2007;579:173–226.
17. Rubinstein I, Zaltzman B. Physical Review E (Statistical, Nonlinear, and Soft Matter Physics) 2005;72:011505.
18. Oddy MH, Santiago JG. Physics of Fluids 2005;17(6):064108–064108-17.
19. Park SY, Russo CJ, Branton D, Stone HA. Journal of Colloid and Interface Science 2006;297(2): 832–839. [PubMed: 16376361]
20. Dong L, Agarwal AK, Beebe DJ, Jiang HR. Nature 2006;442(7102):551–554. [PubMed: 16885981]
21. Park TG, Hoffman AS. Journal of Applied Polymer Science 1992;46(4):659–671.
22. Shin MS, Kang HS, Park TG, Yang JW. Polymer Bulletin 2002;47(5):451–456.
23. Traitel T, Kost J, Lapidot SA. Biotechnology and Bioengineering 2003;84(1):20–28. [PubMed: 12910539]

24. Sørensen, TS.; Dekker, M. Surface chemistry and electrochemistry of membranes. New York: 1999. p. xiip. 1016
25. Mao P, Han JY. Lab on a Chip 2005;5(8):837–844. [PubMed: 16027934]
26. Kim P, Jeong HE, Khademhosseini A, Suh KY. Lab on a Chip 2006;6(11):1432–1437. [PubMed: 17066166]
27. Kim SJ, Han JY. Analytical Chemistry 2008;80(9):3507–3511. [PubMed: 18380489]
28. Yildiz B, Isik B, Kis M, Birgul O. J. Appl. Polym. Sci 2003;88(8):2028–2031.
29. Kim D, Beebe DJ. Lab on a Chip 2007;7(2):193–198. [PubMed: 17268621]
30. Dhopeshwarkar R, Li SA, Crooks RM. Lab on a Chip 2005;5(10):1148–1154. [PubMed: 16175272]
31. Dhopeshwarkar R, Crooks RM, Hlushkou D, Tallarek U. Analytical Chemistry 2008;80(4):1039–1048. [PubMed: 18197694]
32. Rubinstein I, Shtilman L. Journal of Chemical Society Faraday Transactions II 1979;75:231–246.
33. Mani A, Zangle TA, Santiago JG. Langmuir 2009;25:3898–3908. [PubMed: 19275187]
34. Zangle TA, Mani A, Santiago JG. Langmuir 2009;25:3909–3916. [PubMed: 19275188]
35. Pu Q, Yun J, Temkin H, Liu S. Nano Lett 2004;4:1099–1103.
36. Stroock AD, Weck M, Chiu DT, Huck WTS, Kenis PJA, Ismagilov RF, Whitesides GM. Physical Review Letters 2000;84(15):3314–3317. [PubMed: 11019078]
37. Rubinstein I, Zaltzman B. Phys. Rev. E 2000;62:2238–2251.
38. Xia YN, Kim E, Whitesides GM. Chem. Mater 1996;8(7):1558–1567.

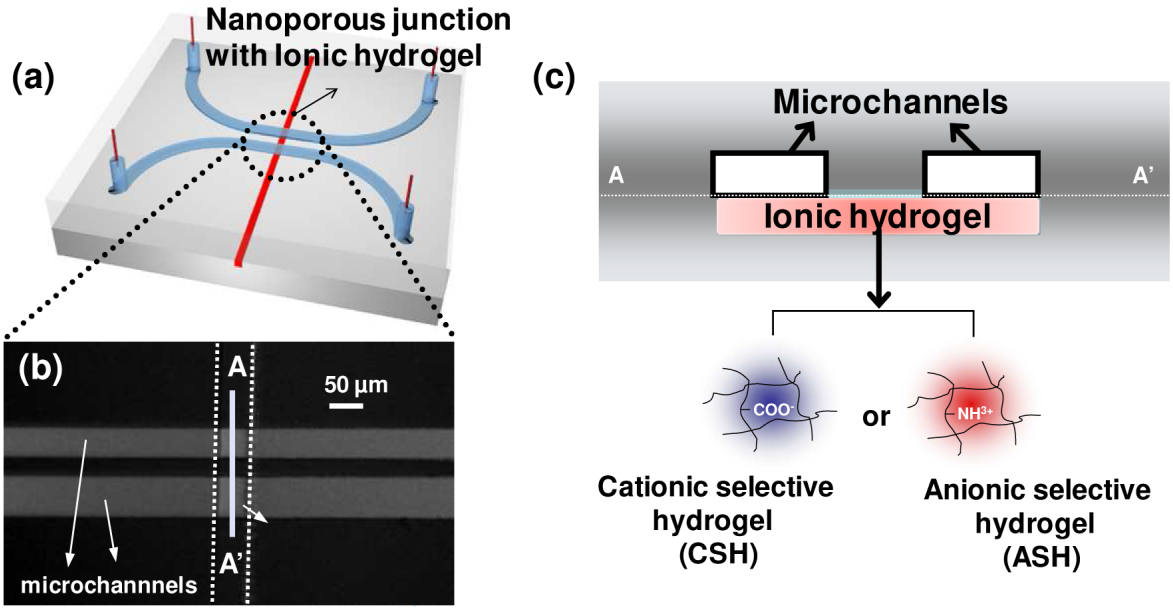

Figure 1.

Fabrication of a nanoporous junction hybrid device with ionic hydrogels. (a) optical micrograph showing the top view of the hybrid device, and (b) its cross section at the location indicated by A-A'. Cationic selective hydrogel (CSH, fixed group: $-COO^{-}$) and anionic selective hydrogel (ASH, fixed group: $-NH^{3+}$) were used for the hybrid device.

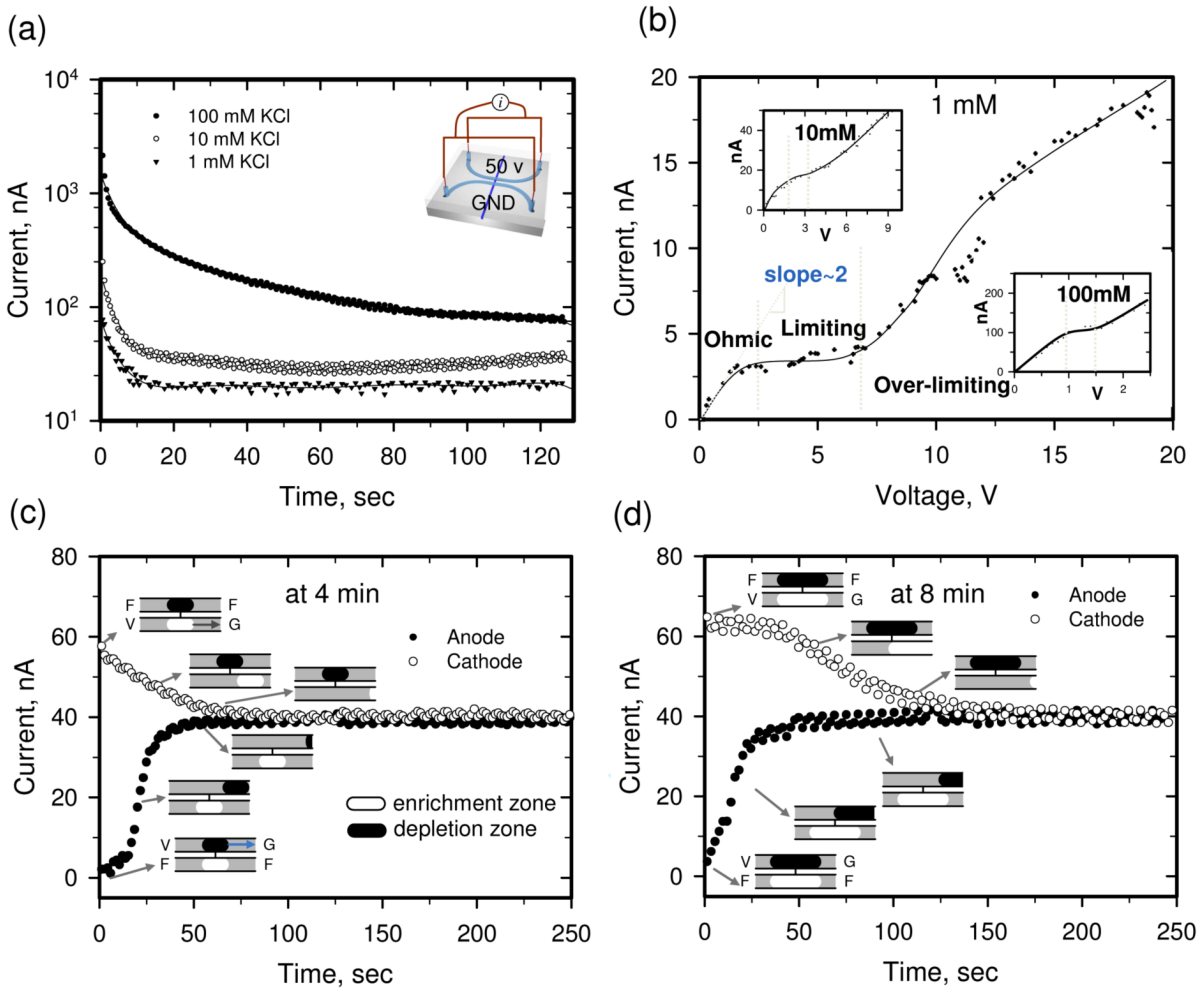

Figure 2.

Ionic current measurement of the CSH junction. (a) Ion current density through nanoporous – junction for various ion concentration (buffer concentration) (b) Current sweep plot showing the limiting current and overlimiting current pattern for three different concentrations. The voltage sweep was done by a programmed voltage source (current-source measurement unit 236, Keithley Instruments, Inc., OH). The voltage was ramped from 0 to 20 V, 0.1 V / 30sec. Plot of ion current through each microchannel for investigating the formation of ion-depletion / enrichment zone after maintaining voltage through nano-junction for 4 minutes (c) and 8 minutes (d) (V: voltage, G: electrical ground and F: electrical floating). 1 mM KCl buffer solution was used for (c) and (d).

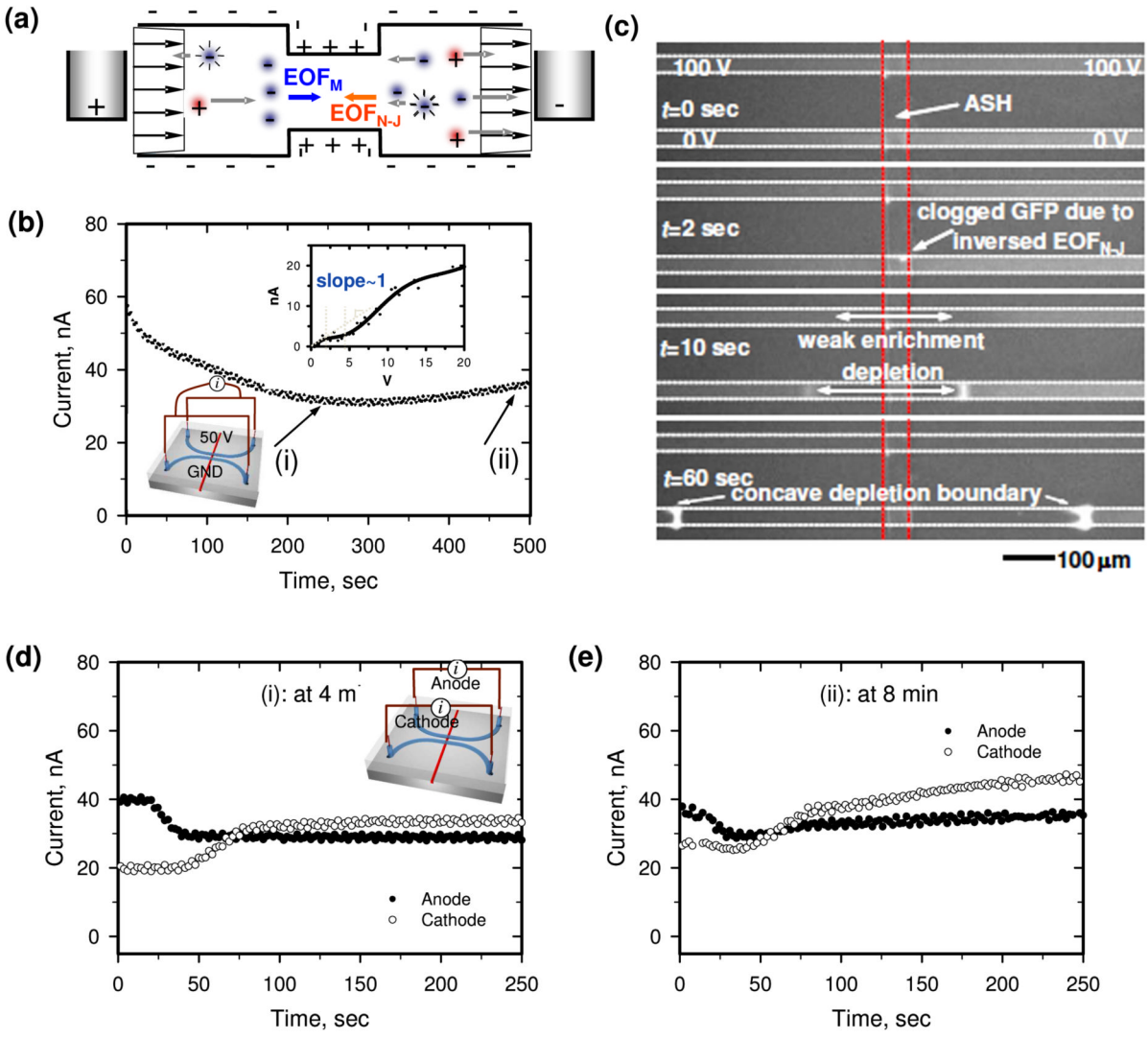

Figure 3.

Ionic current measurement and fluorescent tracking of the ASH type junction. (a) Schematic illustration of EOF through nanoporous junctions. (b) Ion current through ASH junction as a function of time. (c) Fluorescent image tracking of ion depletion / ion enrichment zone in ASH system as a function of time. (d) and (e) Plot of ion current through each microchannel to investigate the formation of ion- depletion / enrichment zones after maintaining voltage through the nanoporous junction for 4 minutes (d) and 8 minutes (e). (Also, see Supplemental Movie 1) 1 mM KCl buffer solution was used.

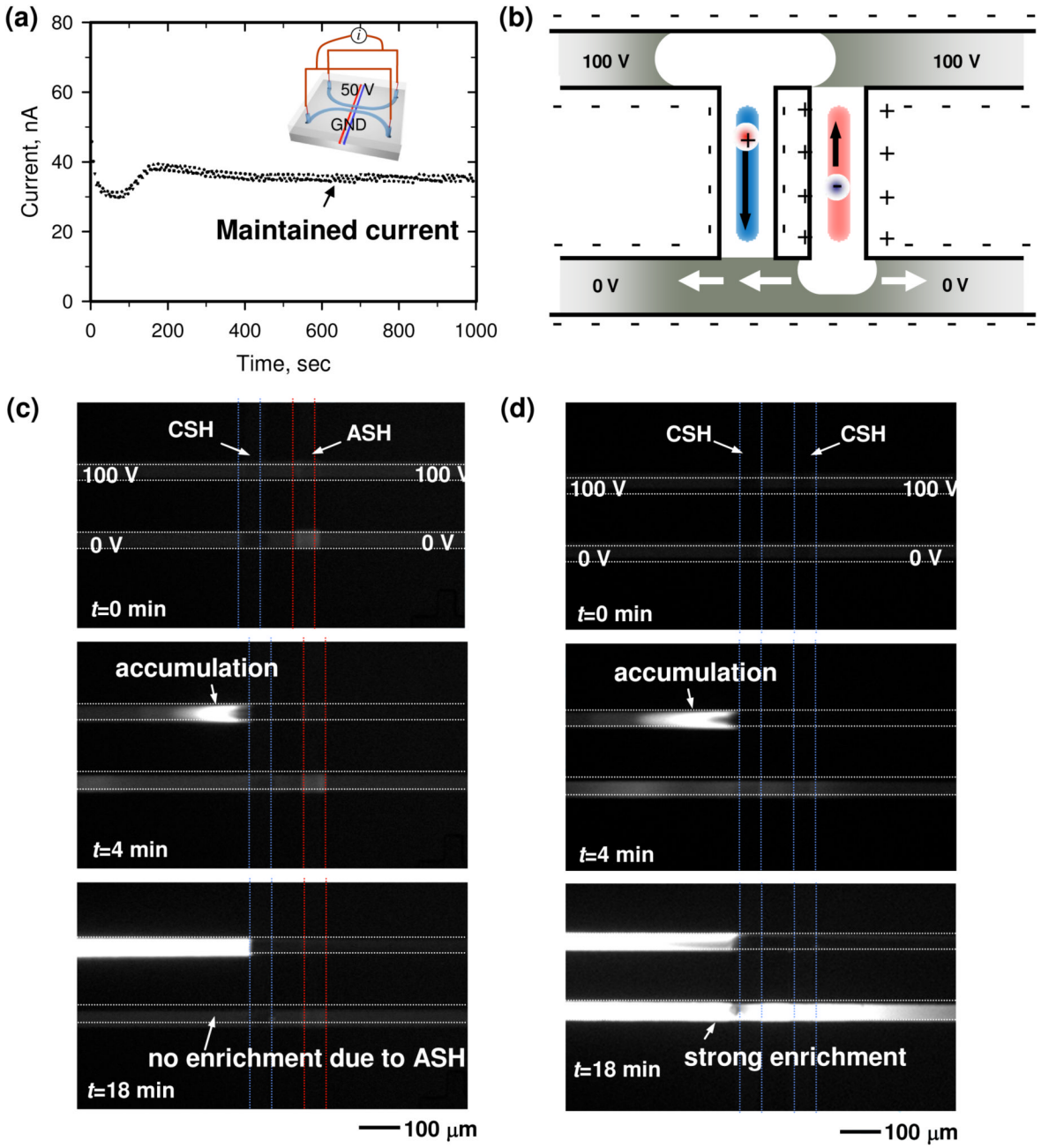

Figure 4.

Ion movement of the ASH-CSH hybrid junction. (a) Ion current through the ASH-CSH junction as a function of time. (b) Schematic illustration of ion transport through the ASH-CSH hybrid system. Experimental observation of ion transport through ASH-CSH hybrid system (c) and CSH-CSH (d). The ion enrichment zone at the cathodic side of CSH junction disappears due to strong ion depletion from the ASH junction. (Also, see Supplemental Movie 2 and Movie 4) 1 mM KCl buffer solution was used.

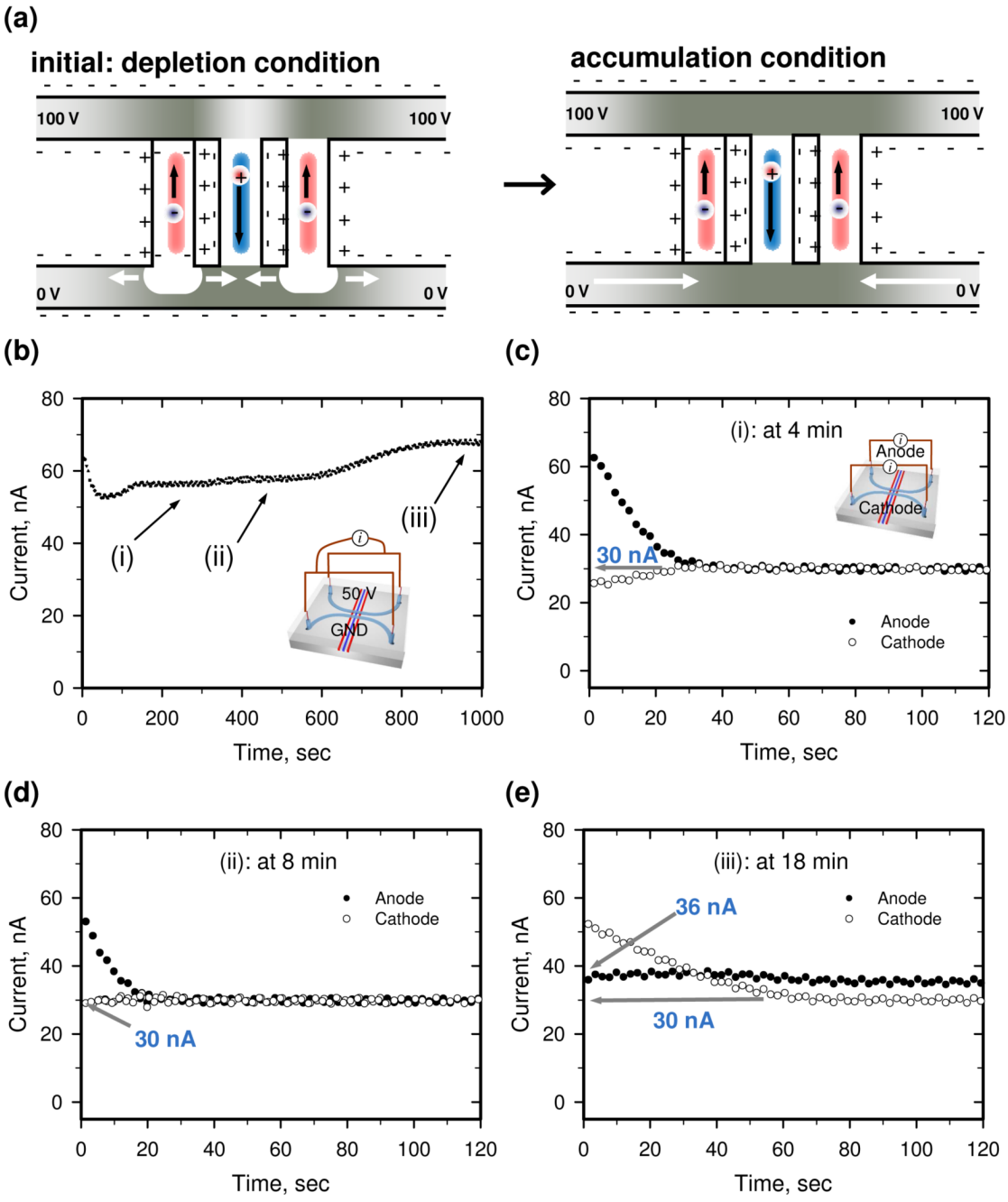

Figure 5.

Ionic current measurement of the ASH-CSH-ASH hybrid junction. (a) Schematic illustration of ion transport through ASH-CSH hybrid system (b) Ion current through the ASH-CSH-ASH hybrid junction as a function of time. (c-e), Plot of ion current through each microchannel to investigate the formation of ion- depletion / enrichment zones after maintaining voltage through the nanoporous junction for 4 minutes (c), 8 minutes (d) and 18 minutes (e). 1 mM KCl buffer solution was used.